Cellulose (2014) 21:1553–1559
DOI 10.1007/s10570-014-0180-z

ORIGINAL PAPER

Dispersion stability and aggregation behavior of TEMPO-oxidized cellulose nanofibrils in water as a function of salt addition

Hayaka Fukuzumi · Reina Tanaka · Tsuguyuki Saito · Akira Isogai

Received: 19 November 2013 / Accepted: 22 January 2014 / Published online: 30 January 2014
© Springer Science+Business Media Dordrecht 2014

Abstract Dispersion stability of TEMPO-oxidized cellulose nanofibrils (TOCNs) in water was investigated through both experimental and theoretical analyses to elucidate the critical aggregation concentration of different salts. The 0.1 wt% TOCN/water dispersions with various NaCl concentrations were evaluated by measuring light transmittance, viscosity under steady-shear flow, and the weight fraction of TOCN that had aggregated. Homogeneous TOCN/water dispersion turned to gel as the NaCl concentration increased. The TOCN dispersion maintained its homogeneous state up to 50 mM NaCl, but aggregated gel particles were formed at 100 mM NaCl. The mixture became separated into two phases (gel and supernatant) at $\geq$200 mM NaCl. Theoretical analysis using ζ-potentials of TOCN elements in the dispersions revealed that the aggregation behavior upon NaCl addition could be explained well in terms of the interaction potential energy between two cylindrical rods based on the Derjaguin–Landau–Verwey–Overbeek theory. The experiments were extended to analyze critical aggregation concentrations of $MgCl_2$ and $CaCl_2$ for the 0.1 wt% TOCN dispersion. In the case of divalent electrolytes, TOCN elements began to form aggregated gel particles at salt concentrations of 2–4 mM, corresponding to the critical aggregation concentration predicted by the empirical Schultz-Hardy rule.

Keywords TEMPO-oxidized cellulose nanofibril · DLVO theory · Critical aggregation concentration · Schulz–Hardy rule

H. Fukuzumi · R. Tanaka · T. Saito · A. Isogai (✉)
Department of Biomaterials Science, Graduate School of Agricultural and Life Sciences, The University of Tokyo, 1-1-1 Yayoi, Bunkyo-ku, Tokyo 113-8657, Japan
e-mail: aisogai@mail.ecc.u-tokyo.ac.jp

Introduction

Nanocelluloses have been attracting much attention as sustainable materials for nano-reinforcing elements of polymer composites, rheology-controlling agents, high performance hydrogels, aerogels, filters, and gas-barrier films (Siró and Plackett 2010; Klemm et al. 2011; Isogai et al. 2011; Saito et al. 2011; Nemoto et al. 2012; Lavoine et al. 2012). Cellulose nanocrystals (CNCs) are rod-like whiskers with relatively low aspect ratios; their widths and lengths are 5–10 and 100–250 nm, respectively (Klemm et al. 2011; Dong et al. 1998). Nanofibrillated celluloses (NFCs) have higher aspect ratios; width range of 3–100 nm and lengths from hundreds of nanometers to several micrometers (Siró and Plackett 2010; Klemm et al. 2011; Isogai et al. 2011; Syverud and Stenius 2009). In NFC preparation, a chemical pretreatment, such as partial carboxymethylation or oxidation, is applied to wood cellulose fibers to bestow additional surface charges on the NFC surfaces. This then enables the preparation of sufficiently nano-dispersed NFCs by

mechanical disintegration of the pre-treated cellulose fibers in water, and reduces the amount of energy required for fibrillation (Klemm et al. 2011; Isogai et al. 2011). In particular, oxidation with 2,2,6,6-tetramethylpiperidine-1-oxyl radical (TEMPO) gives high anionic surface charges with high densities (1.7 glucose units/nm^2) arising from dissociated C6-carboxyl groups formed on the fibril surface (Isogai et al. 2011). The TEMPO-oxidized cellulose fibrils (TOCNs) thus prepared from wood cellulose fibers have homogeneous widths of $\sim$3 nm, the crystal width for intact wood cellulose microfibrils. Thus, TOCNs have high surface-anionic charges, and small and homogeneous widths.

To clarify the fundamental properties of TOCNs and to exploit their advantageous points, complete individualization of TOCNs in aqueous dispersions, without any aggregates or agglomerates, should be achieved. Aggregation of TOCN elements in dispersion leads to a decrease in light transmittance and that in light transparency of TOCN films prepared thereof. Colloidal stability of nanocelluloses in water has been studied in terms of electrostatic repulsion of surface-charged groups and Van der Waals attractive energy based on the Derjaguin–Landau–Verwey–Overbeek (DLVO) theory. This theory explains that chemical factors, such as pH and electrolyte concentration, can decrease the thickness of the electrical double layers of colloids and bring about aggregation of colloids through Brownian motion. Boluk et al. (2011, 2012) applied this theory to analyze the stability of surface-sulfated CNC dispersions. The interactions between NFCs in ionic solutions have been studied by Wågberg et al. (2008), and this study was extended by Fall et al. (2011) using carboxymethylated NFCs and enzymatically-pretreated NFCs. However, the stability of nano-dispersions of highly surface-charged TOCNs has not yet been theoretically studied. It has been reported that TOCNs can be stably nano-dispersed in water at pH $\geq$ 4 (Qi et al. 2012). However, no study has been reported on the stability of aqueous TOCN dispersions as a function of electrolyte concentration.

In this study, the influence of salt concentration on the dispersion stability of a 0.1 % TOCN/water dispersion was investigated to elucidate critical aggregation concentrations for different salts. The experimentally obtained values were compared with those calculated based on the conventional DLVO theory.

Experimental

Preparation of salt-containing TOCN/water dispersions

A commercially available softwood breached kraft pulp for papermaking (Nippon Paper Co., Ltd., Tokyo, Japan) was used as the original wood cellulose. The SBKP was soaked in 0.1 M HCl at room temperature for 2 h for demineralization, and then washed through repeated filtration with water. The fibrous wood cellulose was oxidized in water at pH 10 and room temperature using the TEMPO/NaBr/NaClO system with 10 mmol NaClO/g-cellulose, and further oxidized with $NaClO_2$ in water at pH 4–5 for 44 h to convert a small amount of C6-aldehydes in the oxidized cellulose to C6-carboxylates (Shinoda et al. 2012). The TEMPO-oxidized cellulose thus obtained was thoroughly washed through filtration with water. A 0.1 wt% aqueous slurry of the TEMPO-oxidized cellulose was disintegrated by sonication for 8 min using an ultrasonic homogenizer (US-300T; Nihonseiki Kaisha Ltd., Japan). Before the sonication treatment, the pH of the slurry was adjusted to 8 with 0.05 M NaOH. The TOCN dispersion thus obtained was centrifuged to remove a small unfibrillated fraction (<5 %), and the supernatant was used as the TOCN/water dispersion in the following experiments. The conductivity and pH of the 0.1 % TOCN/water dispersion thus prepared were 10 μS/cm and 7.2, respectively. The carboxylate content and morphology of the TOCN were measured by conductometric titration (Saito and Isogai 2004) and atomic force microscopy (AFM) (Boluk et al. 2011), respectively. Added salts were of laboratory grade (Wako Pure Chemicals, Tokyo, Japan), and used without further purification. Suitable amounts of NaCl, $MgCl_2$, and $CaCl_2$ were added to the 0.1 % TOCN/water dispersions to adjust the salt concentrations, and the dispersions were vigorously stirred for 30 min, and then allowed to stand for 1 h before analysis.

Evaluation of dispersion stability of TOCN

The stability of the TOCN/water dispersions against salt addition was evaluated based on their light transmittances at a wavelength of 546 nm, viscosities under steady-shear flow, and weight fractions of aggregated TOCN gel. The light transmittance was measured using

a UV–vis absorption spectrometer (V-670; JASCO Co., Japan). The shear viscosity measurement was carried out at 25 °C using a stress-controlled rheometer equipped with a 2° cone plate fixture 50 mm in diameter (MCR; Anton Paar GmbH, Austria) with a vapor trap to prevent evaporation. The shear rate was set from 1 to 100/s and increased logarithmically. At each shear rate, the dispersion was held for sufficiently long time (∼1 h) to stabilize the shear flow before recording the shear viscosity. The weight fraction of aggregated TOCN gel was calculated as follows. The salt-containing TOCN/water dispersions (5 mL each) containing 5 mg TOCN were centrifuged at 12,000×*g* for 20 min. The gel particle fraction in the dispersion was washed repeatedly with water by centrifugation three times to remove the salt. The gel particle fraction was freeze-dried and its dry weight was measured. The weight fractions of aggregated TOCN gel were expressed as percentages based on the TOCN weight (5 mg) initially present in the dispersions.

Analyses

A 10-μL drop of the 0.1 % TOCN/water dispersion was placed on a freshly cleaved mica surface (∼1 cm square). One minute later, the excess liquid was carefully blown with air, and the mica surface was rinsed with water. The mica surface was blown with air again until no liquid remained. The AFM measurement was conducted within 30 min of sample preparation. A multimode Nanoscope AFM (Veeco Ltd, USA) with a Veeco RTESP tip was used for capturing images in tapping mode at a resonance frequency of 300 kHz. The tip had a radius of <10 nm and a spring constant of 40 N/m. The tip was oscillated at a 5 % offset in relation to its resonance frequency. ζ-Potentials of the TOCN/water dispersions at different salt concentrations were determined at 25 °C using a DelsaNano HC Particle Analyzer (Beckman Coulter Inc., USA). The measurement was carried out for 0.1 % TOCN/water dispersions in 10–400 mM NaCl.

Results and discussion

Stability of 0.1 % TOCN/water dispersion to NaCl addition

The TOCN prepared in this study had a carboxylate content of 1.5 mmol/g, an average nanofibril width of 3.1 ± 0.6 nm, a length-average length (L_n) of 280 ± 180 nm, and a length-weighted average length (L_w) of 390 nm. The lengths of TOCN elements were measured from AFM images, which were corrected using TOCN widths and heights observed by AFM, to exclude the effect of the cantilever tip width. In total, 56 TOCN elements were observed using AFM for statistical calculations. The L_n and L_w were calculated in a similar manner to that used for the number- and weight-average molecular weights of polymers. The 0.1 wt% TOCN dispersion can be regarded as a semi-dilute solution of rigid rod-like particles (Wierenga and Philipse 1998; Bercea and Navard 2000; Solomon and Spicer 2010). According to the results recently obtained in our laboratory, critical aggregation concentrations (c*) of dilute and semi-dilute TOCN dispersions varied, depending on the TOCN lengths. The c* value of the TOCN with L_w of 440 nm was 0.06 wt% based on shear-viscosity values (Tanaka et al., unpublished data).

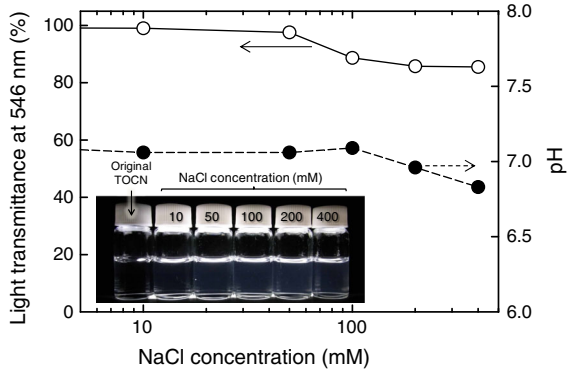

Fig. 1 Light transmittance and pH of 0.1 % TOCN/water dispersions with various NaCl concentrations. *Inset* is a photograph of the dispersions

The aggregation behavior of TOCN elements and the critical aggregation concentration were experimentally investigated using three procedures. First, light transmittances of the 0.1 % TOCN/water dispersions containing NaCl were measured to evaluate the amounts of gel particles formed by the NaCl addition (Fig. 1). As shown in the inset in Fig. 1, all the dispersions were visually transparent and had quite low turbidities, even at high salt concentrations. However, the light transmittance significantly decreased from 99 to 85 % as the NaCl concentration increased from 0 to 400 mM. In particular, a notable change was observed between 50 and 200 mM NaCl;

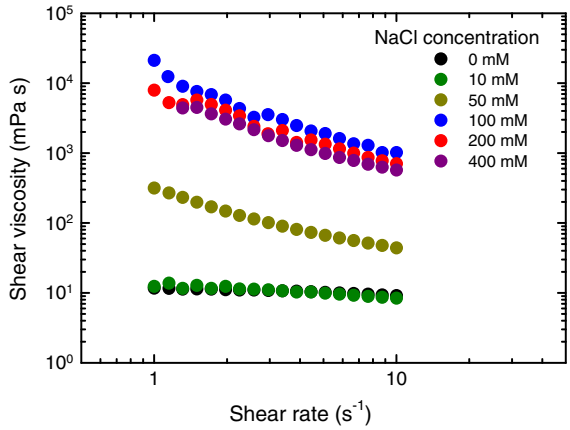

Fig. 2 Shear viscosity of 0.1 % TOCN/water dispersions with various NaCl concentrations

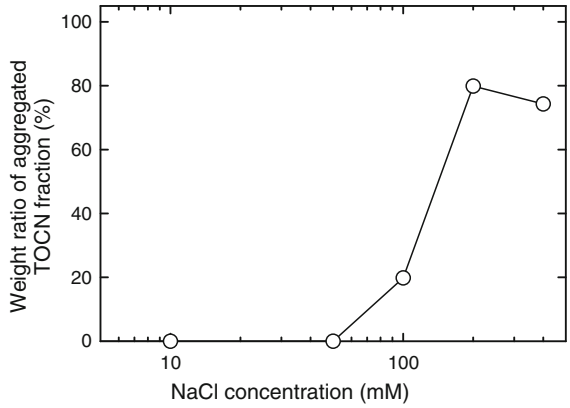

Fig. 3 Weight fraction of aggregated TOCN gel as a function of NaCl concentration in 0.1 % TOCN/water dispersion

TOCN elements clearly formed aggregates or agglomerates between these NaCl concentrations, resulting in the increase in light scattering. The pH of the dispersions was almost unchanged from 0 to 100 mM NaCl, and slightly decreased at 200 and 400 mM.

Second, shear viscosities of the TOCN/water dispersions were measured to evaluate aggregation or gelation behavior (Fig. 2). All the TOCN/water dispersions showed the non-Newtonian and shear-thinning fluid nature previously reported for NFC dispersions (Pääkkö et al. 2007; Crawford et al. 2012). The shear viscosity increased up to an NaCl concentration of 100 mM and then decreased at 200 and 400 mM. These results indicated that the homogeneous TOCN dispersion gradually changed into one containing gel particles with increasing as the salt concentration increased up to 100 mM NaCl. Clear phase separation between the TOCN gel particles and supernatant was observed at 200 and 400 mM NaCl.

Third, the TOCN gel particles were recovered after washing with water for demineralization, and the weight fractions of the aggregated TOCN gel particles were estimated (Fig. 3). Aggregated TOCN gel particles began to form at 100 mM NaCl, and 80 % of TOCN elements were recovered as gel particles from the dispersion containing 200 mM NaCl. Thus, the stability of the 0.1 % TOCN/water dispersion was clearly affected by the NaCl concentration. The TOCN elements were stably nano-dispersed in water at NaCl concentrations of ≤50 mM, but the TOCN dispersion lost its fluidity and partial gelation took place at NaCl concentrations ≥100 mM.

Colloidal stability of TOCN, based on DLVO theory

The interaction potential energy V between colloidal particles in a dielectric solvent is generally expressed by the following equation based on the DLVO theory,

$$V = V_R + V_A \tag{1}$$

where V_R is the repulsive potential energy, and V_A is the attractive van der Waals potential energy. For theoretical analysis of the TOCN used in this study, the TOCN elements were regarded as cylindrical rods with radius a of 1.5 nm and length L of 390 nm (refer to the first paragraph of the "Results and discussion" section). The potentials for two parallel V^P and crossed V^C cylindrical rods are given by the following equations proposed by Israelachvili (2011).

$$V_R^P = 64\pi^{0.5}\frac{(\kappa a)^{0.5}}{\kappa^2}nkT\gamma^2 L\exp(-\kappa H) \tag{2}$$

$$V_A^P = \frac{-ALa^{0.5}}{24H^{1.5}} \tag{3}$$

$$V_R^C = 128\pi\frac{a}{\kappa^2}nkT\gamma^2\exp(-\kappa H) \tag{4}$$

$$V_A^C = \frac{-Aa}{6H} \tag{5}$$

$$\gamma = \tanh\left(\frac{e\psi_0}{4\kappa t}\right) \tag{6}$$

Table 1 Debye length κ^{-1} and ζ-potential of TOCN elements in 0.1 % aqueous dispersions of various NaCl concentrations

NaCl concentration (mM)	κ^{-1} (nm)	ζ-potential (mV)
10	3.04	−37.39
50	1.36	−34.34
100	0.961	−25.70
200	0.680	−15.69
400	0.481	−14.96

$$\kappa = \sqrt{\frac{2\rho e^2}{\varepsilon_0 \varepsilon kT}} \tag{7}$$

where H is the distance between particles, n is the number density of ions, k is the Boltzmann constant, T is the absolute temperature, κ is the reciprocal Debye length in the presence of salt with the cation/anion electrolyte molar ratio of 1:1 such as Na^+Cl^-, ψ_0 is the surface potential of particles, e is the electron charge, A is the Hamaker constant, ρ is the bulk concentration of electrolyte, ε_0 is the vacuum permittivity, and ε is the relative permittivity. Although these equations strictly apply in the range of $a \gg H$ and our case ($a = 1.5$ nm) does not meet this criterion, the colloidal stability of TOCN elements has been previously explained using DLVO theory in other situations where $a \gg H$ is not true (Boluk et al. 2011, 2012; Wågberg et al. 2008; Fall et al. 2011). The V values of the TOCN/water dispersion containing NaCl were calculated approximating the surface potential of TOCN as its ζ-potential, and using $A = 3.5 \times 10^{-21}$ J (Notley et al. 2004). The Debye lengths calculated from Eq. (7) and the ζ-potentials of TOCN elements in 0.1 % TOCN/water dispersions of 10–400 mM NaCl are listed in Table 1.

Figure 4 shows the interaction energies (V) between two cylinders in parallel and crossed orientations. The two cylinders have to overcome the maximum potential (V_{max}) to approach each other in these directions. In other words, the two cylinders cannot approach each other only by Brownian motion, and maintain a stable dispersion state without aggregation, when the magnitude of V_{max} is sufficiently higher than kT (Araki 2013). At NaCl concentrations of below 50 mM, the V_{max} of the TOCN elements is sufficiently high in both parallel and crossed orientations, indicating that repulsive forces predominantly affect the TOCN elements and thus lead to high nano-

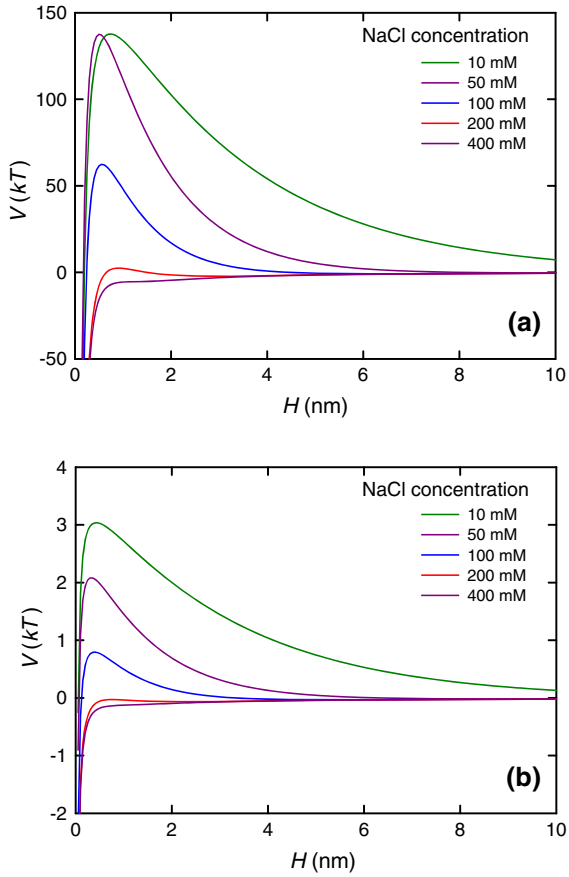

Fig. 4 Interaction potential energy (V) between two cylinders in parallel (**a**) and crossed (**b**) orientations

dispersibility. At 100 mM NaCl, the V_{max} for the parallel orientation is above 50 kT, but that for the crossed orientation is lower than kT. TOCN elements thus tend to approach each other in a cross-wide fashion by Brownian motion at this concentration. At 200 mM NaCl, the V_{max} for the parallel orientation is around kT, and that for the crossed orientation is lower than 0 kT. Moreover, the V_{max} is negative for both parallel and crossed orientations at 400 mM NaCl. Therefore, TOCN elements easily approach each other and rapidly began to form aggregates at 200 mM NaCl or higher.

The aggregation behavior of TOCN elements described by the DLVO theory corresponded closely to that obtained by the experiments. The critical aggregation concentration of the 0.1 % TOCN/water dispersion was determined to be ∼200 mM NaCl by both experimental and theoretical analyses.

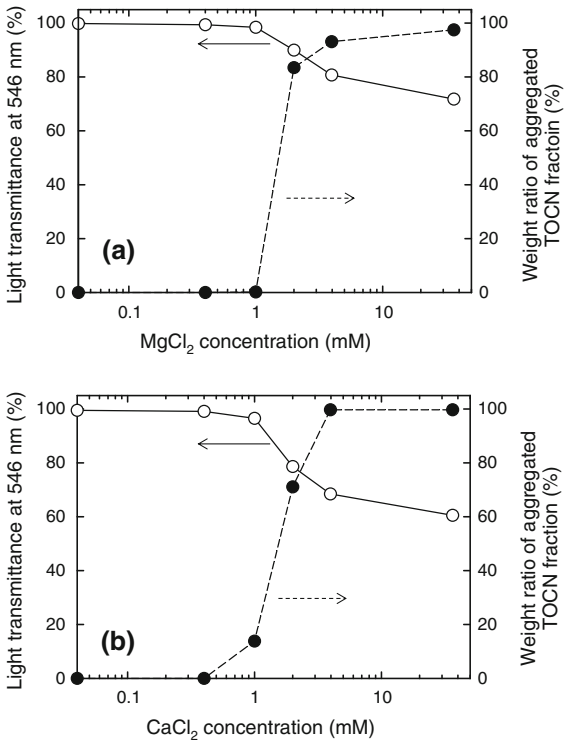

Fig. 5 Light transmittance and weight fraction of aggregated TOCN gel in 0.1 % TOCN/water dispersions with various $MgCl_2$ (**a**) and $CaCl_2$ (**b**) concentrations

Stability of 0.1 % TOCN/water dispersion against $MgCl_2$ and $CaCl_2$

In many colloidal systems, the critical aggregation concentration (ρ_c) of electrolyte correlates inversely with the sixth power of the electrolyte valence (z),

$$\rho_c \propto \frac{1}{z^6} \tag{8}$$

This Eq. (8) is known as the Schultz-Hardy rule (Schulze 1882; Hardy 1899). This was originally an empirical rule, but was later supported theoretically by the DLVO theory (Overbeek 1980). This rule has been observed for many colloids, including peptide nanofibers (Stendahl et al. 2006), single-walled carbon nanotubes (Sano et al. 2001), and microcrystalline celluloses (Rånby 1951; Lindström and Soremark 1976; Kratohvil et al. 1969). According to this rule, the critical aggregation concentration of the 0.1 % TOCN/water dispersion containing divalent electrolytes is predicted to be $\sim$3 mM.

Figure 5 shows the light transmittance and weight fraction of gel in the 0.1 % TOCN/water dispersions containing $MgCl_2$ and $CaCl_2$. The weight increase of the gel fraction of TOCN aggregates owing to ion exchange from Na^+ to Mg^{2+} or Ca^{2+} was not taken into account when calculating the weight fractions of aggregated TOCN gel. In the case of $MgCl_2$, the light transmittance decreased at a salt concentration of 2 mM, and approximately 80 % of TOCN elements were recovered as gel particles at this concentration. When $CaCl_2$ was used, the light transmittance decreased in a similar manner with increasing salt concentration, and began to decrease at 2 mM. Almost 100 % of TOCN elements were recovered as gel particles at 4 mM $CaCl_2$. The estimated critical aggregation concentrations of 2–4 mM the divalent salts with TOCN agreed well with those calculated by the Eq. (8) for both $MgCl_2$ and $CaCl_2$.

Conclusion

Dispersion stability of TOCN elements in water was investigated to elucidate critical salt concentration for aggregation. The obtained light transmittances, viscosities, and weight fractions of aggregated TOCN showed that the stability of the 0.1 % TOCN/water dispersion was affected by NaCl concentration. The TOCN elements were stably nano-dispersed in water at NaCl concentrations $\leq$50 mM. However, the TOCN dispersion gradually lost its fluidity and gelation became remarkable with the increased salt concentration. The TOCN elements partially aggregated in the dispersion at 100 mM NaCl, and, at $\geq$200 mM NaCl, almost all TOCN elements in the dispersions formed aggregated gel particles, resulting in phase separation. This aggregation or gelation behavior could be explained well in terms of the interaction potential energy of two crossed cylindrical rods based on the DLVO theory. When $MgCl_2$ or $CaCl_2$ was used in place of NaCl, the TOCN elements began to form aggregated gel particles at salt concentrations of 2–4 mM, which corresponded well to the critical aggregation concentration calculated based on the Schultz-Hardy rule.

Acknowledgments This research was supported by Grants-in-Aid for Scientific Research (Grants 21228007 and 25-7327) from the Japan Society for the Promotion of Science (JSPS). We

thank Associate Prof. Jun Araki of Shinshu University for helpful advice concerning theoretical calculations.

References

Araki J (2013) Electrostatic or steric?—preparations and characterizations of well-dispersed systems containing rod-like nanowhiskers of crystalline polysaccharides. Soft Matter 9:4125–4141. doi:10.1039/C3SM27514K

Bercea M, Navard P (2000) Shear dynamics of aqueous suspensions of cellulose whiskers. Macromolecules 33:6011–6016. doi:10.1021/ma000417p

Boluk Y, Lahiji R, Zhao L, McDermott MT (2011) Suspension viscosities and shape parameter of cellulose nanocrystals (CNC). Colloid Surf A 377:297–303. doi:10.1016/j.colsurfa.2011.01.003

Boluk Y, Zhao L, Incani V (2012) Dispersions of nanocrystalline cellulose in aqueous polymer solutions: structure formation of colloidal rods. Langmuir 28:6114–6123. doi:10.1021/la2035449

Crawford RJ, Edler KJ, Lindhoud S, Scott JL, Unali G (2012) Formation of shear thinning gels from partially oxidised cellulose nanofibrils. Green Chem 14:300–303. doi:10.1039/C2GC16302K

Dong XM, Revol JF, Gray DG (1998) Effect of microcrystallite preparation conditions on the formation of colloid crystals of cellulose. Cellulose 5:19–32. doi:10.1023/A:1009260511939

Fall AB, Lindström SB, Sundman O, Ödberg L, Wågberg L (2011) Colloidal stability of aqueous nanofibrillated cellulose dispersions. Langmuir 27:11332–11338. doi:10.1021/la201947x

Hardy WB (1899) A preliminary investigation of the conditions which determine the stability of irreversible hydrosols. Proc R Soc Lond A 66:110–125. doi:10.1098/rspl.1899.0081

Isogai A, Saito T, Fukuzumi H (2011) TEMPO-oxidized cellulose nanofibers. Nanoscale 3:71–85. doi:10.1039/C0NR00583E

Israelachvili JN (2011) Intermolecular and surface forces, 3rd edn. Elsevier, USA

Klemm D, Kramer F, Moritz S, Lindström T, Ankerfors M, Gray D, Dorris A (2011) Nanocelluloses: a new family of nature-based materials. Angew Chem Int Ed Engl 50:5438–5466. doi:10.1002/anie.201001273

Kratohvil S, Janauer GE, Matijević E (1969) Coagulation of microcrystalline cellulose dispersions. J Colloid Interface Sci 29:187–193. doi:10.1016/0021-9797(69)90185-4

Lavoine N, Desloges I, Dufresne A, Bras J (2012) Microfibrillated cellulose—Its barrier properties and applications in cellulosic materials: a review. Carbohydr Polym 90:735–764. doi:10.1016/j.carbpol.2012.05.026

Lindström T, Soremark C (1976) Flocculation of cellulosic dispersions with alginates in the presence of divalent metal ions. J Colloid Interface Sci 55:69–72. doi:10.1016/0021-9797(76)90009-6

Nemoto J, Soyama T, Saito T, Isogai A (2012) Nanoporous networks prepared by simple air drying of aqueous TEMPO-oxidized cellulose nanofibril dispersions. Biomacromolecules 13:943–946. doi:10.1021/bm300041k

Notley SM, Pettersson B, Wågberg L (2004) Direct measurement of attractive van der Waals' forces between regenerated cellulose surfaces in an aqueous environment. J Am Chem Soc 126:13930–13931. doi:10.1021/ja045992d

Overbeek JTG (1980) The rule of Schulze and Hardy. Pure Appl Chem 52:1151–1161. doi:10.1351/pac198052051151

Pääkkö M, Ankerfors M, Kosonen H, Nykänen A, Ahola S, Österberg M, Ruokolainen J, Laine J, Larsson PT, Ikkala O, Lindström T (2007) Enzymatic hydrolysis combined with mechanical shearing and high-pressure homogenization for nanoscale cellulose fibrils and strong gels. Biomacromolecules 8:1934–1941. doi:10.1021/bm061215p

Qi ZD, Saito T, Fan Y, Isogai A (2012) Multifunctional coating films by layer-by-layer deposition of cellulose and chitin nanofibrils. Biomacromolecules 13:553–558. doi:10.1021/bm201659b

Rånby BG (1951) Fibrous macromolecular systems. Cellulose and muscle. The colloidal properties of cellulose micelles. Discuss Faraday Soc 11:158–164. doi:10.1039/DF9511100158

Saito T, Isogai A (2004) TEMPO-mediated oxidation of native cellulose. The effect of oxidation conditions on chemical and crystal structures of the water-insoluble fractions. Biomacromolecules 5:1983–1989. doi:10.1021/bm0497769

Saito T, Uematsu T, Kimura S, Enomae T, Isogai A (2011) Self-aligned integration of native cellulose nanofibrils towards producing diverse bulk materials. Soft Matter 7:8804–8809. doi:10.1039/C1SM06050C

Sano M, Okamura J, Shinkai S (2001) Colloidal nature of single-walled carbon nanotubes in electrolyte solution: the Schulze–Hardy rule. Langmuir 17:7172–7173. doi:10.1021/la010698+

Schulze H (1882) Schwefelarsen in wässriger Lösung. J Prakt Chem 25:431–452. doi:10.1002/prac.18820250142

Shinoda R, Saito T, Okita Y, Isogai A (2012) Relationship between length and degree of polymerization of TEMPO-oxidized cellulose nanofibrils. Biomacromolecules 13:842–849. doi:10.1021/bm2017542

Siró I, Plackett D (2010) Microfibrillated cellulose and new nanocomposite materials: a review. Cellulose 17:459–494. doi:10.1007/s10570-010-9405-y

Solomon MJ, Spicer PT (2010) Microstructural regimes of colloidal rod suspensions, gels, and glasses. Soft Matter 6:1391–1400. doi:10.1039/B918281K

Stendahl JC, Rao MS, Guler MO, Stupp SI (2006) Intermolecular forces in the self-assembly of peptide amphiphile nanofibers. Adv Funct Mater 16:499–508. doi:10.1002/adfm.200500161

Syverud K, Stenius P (2009) Strength and barrier properties of MFC films. Cellulose 16:75–85. doi:10.1007/s10570-008-9244-2

Wågberg L, Decher G, Norgren M, Lindström T, Ankerfors M, Axnäs K (2008) The build-up of polyelectrolyte multilayers of microfibrillated cellulose and cationic polyelectrolytes. Langmuir 24:784–795. doi:10.1021/la702481v

Wierenga AM, Philipse AP (1998) Low-shear viscosity of isotropic dispersions of (Brownian) rods and fibres; a review of theory and experiments. Colloid Surf A 137:355–372. doi:10.1016/S0927-7757(97)00262-8

Tanaka R, Saito T, Ishii D, Isogai A, unpublished data